Carbohydrate Polymers 137 (2016) 198–206

Contents lists available at ScienceDirect

Carbohydrate Polymers

journal homepage: www.elsevier.com/locate/carbpol

Organocatalytic route for the synthesis of propionylated starch

S. Di Filippo, M.V. Tupa, A. Vázquez, M.L. Foresti *

Biotechnology and Biosynthesis Group, Institute of Technology in Polymers and Nanotechnology (ITPN), Engineering Faculty, University of Buenos Aires, Las Heras 2214 (CP 1127AAR), Buenos Aires, Argentina

ARTICLE INFO

Article history:
Received 14 September 2015
Received in revised form 10 October 2015
Accepted 10 October 2015
Available online 22 October 2015

Keywords:
Starch
Propionylation
Human colon health
Organocatalytic solventless route

ABSTRACT

In recent years acetylated, propionylated and butyrylated starches have received special attention due to their capacity to deliver specific short chain fatty acids (SCFAs) to the colon in a sustained and predictable manner, and thus contribute to maintaining the normal physiologic function of the large bowel and preventing specific diseases.

In the current contribution a non-conventional organocatalytic solventless route for the eco-friendly propionylation of corn starch is proposed. The catalyst used in the acylation is a naturally occurring α-hydroxy acid (L-tartaric acid). Propionylated starches with degree of substitution (DS) in the 0.05–1.59 interval were obtained and characterized in terms of chemical structure, morphology, crystallinity, thermal stability and hydrophilicity. Results showed that by the proposed methodology propionylated starch with the DS required for clinical use (i.e. 0.2–0.3) could be obtained within 2–3 h of reaction. Characterization results evidenced the progressive loss of crystallinity of starch granules as higher substitution levels were conferred.

1. Introduction

Starch is an abundant, inexpensive and renewable polysaccharide, which is found in storage (grains, tubers, roots) and vegetative tissues of plants deposited as insoluble semi-crystalline granules. Starch plays an important role as functional material in the food and a number of non-food industries. In the food industry, starch is utilized for its various functionalities in thickening, stabilizing, texturizing, gelling, film forming, encapsulation, moisture retention and shelf life extension (Singh, Chawla, & Singh, 2004). On the other hand, non-food uses of starch involve papermaking and adhesives industries, oil exploration (as viscosity modifier of drilling fluids), biodegradable plastics, construction industry (as gypsum binder), and textile industry (as sizing agent of yarns), among others.

However, native OH-rich-hydrophilic starch molecules do not always have the desired properties for certain applications and types of processing. Poor solubility in common organic solvents, substantial swelling, rapid enzymatic degradation, poor mechanical properties and dimensional stability (especially in the presence of water and in humid environments), low shear stress resistance and thermal decomposition, high retrogradation and syneresis, high hygroscopicity, and poor compatibility with hydrophobic media, have all been mentioned as limitations for a wider application of native starch (Bushra et al., 2013; Chi et al., 2008; Diop, Li, Xie, & Shi, 2011; Han, Gao, Liu, Huang, & Zhang, 2013; Wang et al., 2008).

In order to achieve suitable functionalities for various industrial applications, starch can be modified by use of different physical, chemical and enzymatic methodologies (Adebowale, Afolabi, & Lawal, 2002; Betancur, Chel, & Canizares, 1997; Kaur, Ariffin, Bhat, & Karim, 2012). Chemical modifications can promote structural changes and introduce new functional groups that affect the physical and chemical properties of starches (Morán, Cyras, & Vazquez, 2013; Sandhu, Kaur, Singh, & Lim, 2008). Among them, esterification of starch of different botanical origins with a variety of acylating agents have been proposed as effective alternatives for improving starch properties and widening their uses. Esterified starch properties strongly depend on the degree of substitution (DS) conferred, the type of ester groups introduced, and their position within the anhydroglucose molecule.

Among esterified starches, in recent years acetylated, propionylated and butyrylated starches have received special attention due to their reported action as a source of resistant starch (RS) (Annison, Illman, & Topping, 2003; Bajka, 2007; Clarke, Bird, Topping, & Cobiac, 2007; Morita, Kasaoka, Kiriyama, Brown, & Topping, 2005). In general, digestible starches are hydrolyzed by α-amylases, glucoamylase and sucrase–isomaltase enzymes in the small intestine to yield free glucose that is then absorbed (Nugent, 2005). However, there is a fraction of the ingested starch, i.e. resistant starch, which is not digested in the small intestine of healthy humans (Asp,

* Corresponding author.
E-mail address: mforesti@fi.uba.ar (M.L. Foresti).

http://dx.doi.org/10.1016/j.carbpol.2015.10.039
0144-8617/

1992). Instead, resistant starch escapes small intestinal digestion and enters the human large bowel, where it is fermented by the large bowel microflora into short chain fatty acids (SCFA), predominantly acetate, propionate and butyrate (Bajka, 2007). These SCFAs play a key role in the function of epithelial cells and the mucosal barrier in the colon, and maintain an acidic luminal pH that may be beneficial in preventing the production and absorption of potential carcinogens (Cherbut, 2002; Topping & Clifton, 2001).

Among resistant starch sources, starches acylated with acetate, propionate and butyrate groups are of particular interest in view of their capacity to deliver *specific* SCFAs to the colon in a sustained and predictable manner (Annison et al., 2003; Clarke et al., 2007). Starches moderately esterified with SCFAs (i.e. DS 0.2–0.3) are known to resist intestinal digestion and pass to the colon where the esterified fatty acids are liberated by bacterial enzymes (Annison et al., 2003; Morita et al., 2005; West et al., 2013). The residual starch backbone is then fermented with the production of further SCFAs (Clarke et al., 2012; West et al., 2013).

Despite its potentiality in therapeutic and clinical applications, reports on the synthesis of propionylated starch (Annison et al., 2003; Bajka, 2007; Garg & Jana, 2011; López-Rubio, Clarke, Scherer, Topping, & Gilbert, 2009; Santayanon & Wootthikanokkhan, 2003) are scarce. Initial reported methodologies for starch propionylation implied the dissolution of starch in hot DMSO followed by esterification with propionic anhydride and catalyzed by 1-methylimidazole (Annison et al., 2003), or preactivation of starch with pyridine and further esterification with propionic anhydride (Garg & Jana, 2011; Santayanon & Wootthikanokkhan, 2003). However, neither DMSO, nor 1-methylimidazole or pyridine are suitable for the production of food-grade acylated starches (Bajka, 2007). Consequently, later attempts to produce propionylated starches moved to aqueous systems in which starch was slurried in the presence of hydrogen peroxide (to etch the surface of starch granules and facilitate acylation) and aqueous sodium hydroxide to maintain a basic pH (Bajka, 2007; López-Rubio et al., 2009).

Alternatively, in the current contribution, we propose an organocatalytic ecofriendly solvent-free route for the synthesis of propionylated starch with variable DS. The esterification route herein proposed relays on the use as catalyst of L-tartaric acid, a naturally occurring α-hydroxy acid mainly found in grapes, apricots and tamarinds, and industrially produced from by-products of grape juice fermentation in the wine industry. Moreover, neither pre-activation step, nor extra solvent is required. Instead, the acylant (i.e. propionic acid) is used in sufficient excess so as to provide the necessary volume to suspend starch granules. The esterification route proposed has recently proved useful in the preparation of acetylated starches with tunable DS (Tupa, Ávila Ramírez, Vázquez, & Foresti, 2015; Tupa, Maldonado, Vázquez, & Foresti, 2013). However, at the best authors' knowledge there is no previous report on its suitability for the preparation of propionylated starches. Given the importance of knowing the structural characteristics of these acylated starches for later understanding/optimization of SCFA delivery, the obtained esterified starches with varying DS were characterized in terms of morphology, chemical structure and crystallinity. Thermal stability and changes in hydrophilicity of propionylated starch granules were also analyzed.

2. Materials and methods

2.1. Materials

Commercial native corn starch was kindly donated by Ingredion (Argentina). Propionic acid (99.5%) and L(+) tartaric acid were bought from Biopack. All other reagents used, i.e. hydrochloric acid (36.5–38%, Anedra), sodium hydroxide (Biopack), potassium hydrogen phthalate (Laboratorios Cicarelli), petroleum ether 60–80 °C (Laboratorios Cicarelli) and sodium carbonate (Mallinckrodt) were all of analytical grade.

2.2. Organocatalytic propionylation

Propionic acid (25 mL, 333 mmol), L-tartaric acid (3.7 g, 24.6 mmol) and previously dried (105 °C, 2 h) corn starch (2 g, 12.3 mmol AGU) were mixed in an oven-dried 100 mL glass flask equipped with a magnetic stir bar, and a reflux condenser to prevent the loss of the acid. The mixture was then heated to 130 °C in a thermostatized oil bath under continuous agitation. The chosen temperature guaranteed the complete dissolution of tartaric acid in propionic acid and this was considered as the beginning of reaction. Propionylation was run for different reaction times (0.5, 1, 2, 3, 4, 5, 6 and 7 h), in order to inspect the evolution of reaction within this period. After the chosen reaction time, the mixture was allowed to cool down to room temperature, and the solid product was separated by vacuum filtration in a Buchner funnel, followed by several washings with ethanol to guarantee the removal of the catalyst and the unreacted acid. Highly substituted samples required the addition of ethanol (20 mL) into the reaction vial to precipitate the esterified starch. The solid was finally dried at 40–50 °C overnight. Assays were run in duplicate.

2.3. Determination of substitution degree

The degree of substitution (DS) of propionylated starches was determined by heterogeneous saponification and back titration with HCl according to Tupa et al. (2013). Briefly, 0.1 g of dried ground propionylated starch samples were contacted with 20 mL of ethyl alcohol (75%) in 100 mL Erlenmeyer flasks which were heated loosely stoppered during 30 min at 50 °C. Afterwards, the suspensions were brought to slightly basic pH by addition of a few drops of 0.1 N NaOH using phenolphthalein as indicator. 20 mL of 0.1 N NaOH were then added to each flask, and heated again at 50 °C for 15 min. The flasks were finally allowed to stand tightly stoppered at room temperature for 48 h, after which the excess NaOH was back titrated with 0.1 N HCl, using phenolphthalein as endpoint indicator. A blank determination (native corn starch) was carried through the complete procedure. NaOH and HCl solutions were standardized using previously dried standard potassium hydrogen phthalate and sodium carbonate, respectively. The acyl content was then calculated by:

$$\text{Acyl}\quad(\%) = \frac{[(V_B - V_S) \times N_{HCl} \times 5.7]}{W} \tag{1}$$

where V_B (mL) is the volume of HCl required for titration of the blank; V_S (mL) is the volume of HCl required to titrate the sample; N_{HCl} is the normality of the HCl solution, and W (g) is the mass of sample used. Besides, the substitution degree of propionylated starches was calculated by:

$$\text{DS} = \frac{162 \times \text{Acyl}\quad\%}{[5700 - (56 \times \text{Acyl}\quad\%)]} \tag{2}$$

Since the anhydroglucose unit possesses three reactive hydroxyl groups, the maximum DS value (defined as the number of hydroxyl (OH) groups substituted per anhydroglucose unit of the starch polymer) is 3.

2.4. Characterization of starch esters

2.4.1. Solid-state ^{13}C CP-MAS NMR spectroscopy

High-resolution ^{13}C solid-state spectra of grinded samples were recorded using the ramp $\{^1H\} \rightarrow \{^{13}C\}$ CP/MAS pulse sequence

(cross-polarization and magic angle spinning) with proton decoupling during acquisition. All experiments were performed at room temperature in a Bruker Avance II-300 spectrometer equipped with a 4-mm MAS probe. The operating frequency for protons and carbons was 300.13 and 75.46 MHz, respectively. Glycine was used as an external reference for the ^{13}C spectra and to set the Hartmann–Hahn matching condition in the cross-polarization experiments. The recycling time varied from 5 to 6 s according to the sample. The contact time during CP was 2 ms for all of them. The SPINAL64 sequence (small phase incremental alternation with 64 steps) was used for heteronuclear decoupling during acquisition with a proton field H1H satisfying $\omega 1H/2\pi = YHH1H = 62$ kHz. The spinning rate for all the samples was 10 kHz.

2.4.2. Fourier transform infrared spectroscopy (FTIR)

Fourier transform infrared spectra of native and propionylated starches were acquired on an IR Affinity-1 Shimadzu Fourier transform infrared spectrophotometer in transmission mode. Carefully dried (105 °C, 2 h) powdered samples were mixed with KBr in a 1:20 ratio, and spectra were collected with 40 scans in the range of 4000–600 cm^{-1} with a resolution of 4 cm^{-1}. Spectra were normalized using the signal at 1025 cm^{-1} which belongs to the stretching vibration of the acetal of the AGU (anhydroglucose unit), and which does not change with the DS (Hampe & Heinze, 2014).

2.4.3. Scanning electron microscopy (SEM)

Drops of propionylated starch/water suspensions were deposited on microscope glasses and dried at 40 °C for 15 min. Samples were then coated with gold using an ion sputter coater, and observed at a magnification range of 5 and 10 KX by use of a scanning electron microscope Zeiss Supra 40 with field emission gun operated at 3 kV.

2.4.4. X-ray diffraction measurements (XRD)

The structure of dried samples (105 °C, 2 h) of native and propionylated starch was analyzed with a D/Max-C Rigaku automated wide-angle powder X-ray diffractometer, operating at 40 kV and 30 mA, with Cu/Kα radiation (λ = 0.154 nm). X-ray diffraction diagrams were recorded in a 2θ angle range of 10–45° with a step of 0.02° and at a rate of 0.6°/min.

2.4.5. Thermogravimetric analysis (TGA)

Thermogravimetric analysis of dried samples (5.5–6 mg, 105 °C, 2 h) was conducted in a TGA-50 Shimadzu instrument. Temperature programmes were run from 25 °C to 800 °C at a heating rate of 10 °C/min, under nitrogen atmosphere (30 mL/min) in order to prevent thermoxidative degradation.

2.4.6. Hydrophobicity test

Native starch and propionylated starch samples (5 ± 0.5 mg) were qualitatively tested for hydrophobicity by placing them into transparent test tubes containing two immiscible liquid phases, i.e. 1.5 mL of petroleum ether (upper phase) and 1.5 mL of distilled water (lower phase). Depending on their DS, samples distributed preferentially in one of the liquid phases.

3. Results and discussion

3.1. L-Tartaric acid-catalyzed propionylation of starch

Propionylated corn starch samples with varying DS were prepared by tuning the acylation time interval. Fig. 1 illustrates the evolution of the esterification when using propionic acid as acylant and L-tartaric acid as catalyst. No extra solvent was necessary, since propionic acid was added in sufficient excess to suspend starch granules. Under the reaction conditions chosen, tuning the reaction interval (0.5–7 h) allowed obtaining propionylated starches with substitution degree within the 0.05–1.59 range. As previously introduced, acylation of starch to a DS of 0.2–0.3 with acetate, propionate, or butyrate groups has been reported as an effective means of delivering specific SCFA to the large bowel (Annison et al., 2003; Bajka, 2007). By use of the organocatalytic methodology herein proposed, propionylated starches with the required DS could be obtained within 2–3 h of reaction, a time interval much lower than those previously reported for other synthetic routes (Annison et al., 2003; Garg & Jana, 2011; Santayanon & Wootthikanokkhan, 2003).

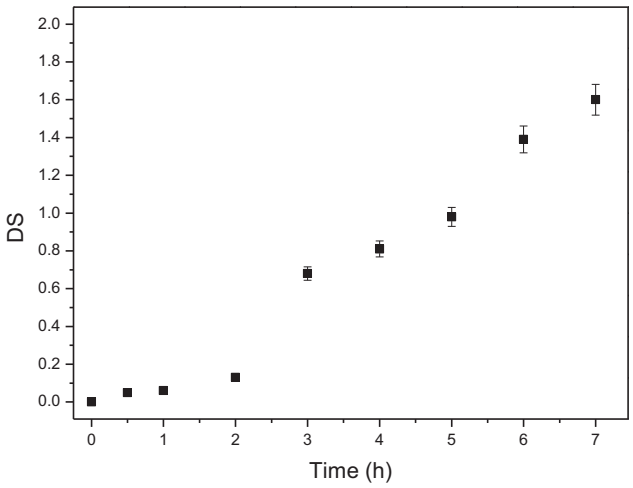

Fig. 1. Evolution of L-tartaric acid catalyzed propionylation of corn starch.

3.2. Solid-state ^{13}C CP-MAS NMR spectroscopy

Propionylation of starch by the proposed organocatalytic methodology was confirmed by use of ^{13}C CP-MAS NMR spectroscopy. Fig. 2 shows the spectra obtained for native and propionylated (DS = 0.98) starch.

Native starch spectrum (Fig. 2a) showed carbon resonances typical of starch, including C1 signals in the 91–107 ppm range, the peak centred at 82 ppm assigned to amorphous C4 carbons, the highly overlapped C2, C3 and C5 lines shown in the 65–80 ppm range, and the resonance of C6 in the 56–65 ppm interval (Paris,

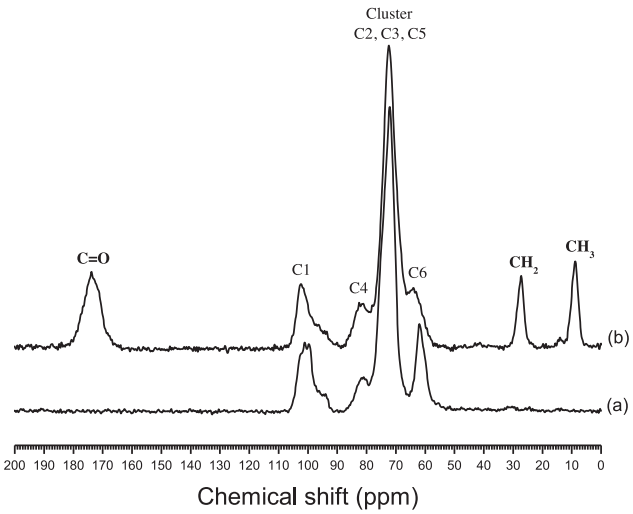

Fig. 2. Solid-state ^{13}C CP-MAS NMR spectra of (a) native and (b) propionylated corn starch (DS = 0.98).

Bizot, Emery, Buzaré, & Buléon, 1999, 2001; Shin, Lee, Kim, Choi, & Kim, 2009, Tang & Hills, 2003). The shoulder centred at 94 ppm has previously been assigned to constrained conformations (Paris et al., 2001). The multiplicities and the chemical shifts assigned to C1 atoms have previously been correlated to the conformation and polymorphisms of starch (Paris et al., 1999); with C1 showing a distinct three-peaks pattern for A-type starch, a two-peaks pattern for B-type starch, a mixed A- and B-type pattern for C-type starch, and a single resonance for V-type starch (Tang & Hills, 2003). C1 lines centred at 102.4 ppm, 101.1 ppm (maximum), and 99.7 ppm in Fig. 2a indicate an A-type polymorphism typical of cereal starch.

Propionylated starch spectrum (Fig. 2b) showed several new resonances, including the peak centred at 173 ppm assignable to the resonance of the carbonyl ester peak of propionate, the new signal centred at 27 ppm assignable to CH_2, and the peak centred at 9 ppm from the resonance of CH_3 of propionate groups. The pattern for C1 with reduced multiplicity and a maximum at 102.4 ppm suggested a reduction in crystalline material upon acylation.

3.3. Fourier transform infrared spectroscopy (FTIR)

The FTIR spectra of propionylated starches were obtained for increasing reaction times and corresponding DS values. Data are shown in Fig. 3a in comparison with the infrared spectrum of unmodified starch. Native starch showed characteristic bands of the polysaccharide, i.e. a abroad band between 3700 and 3000 cm^{-1}

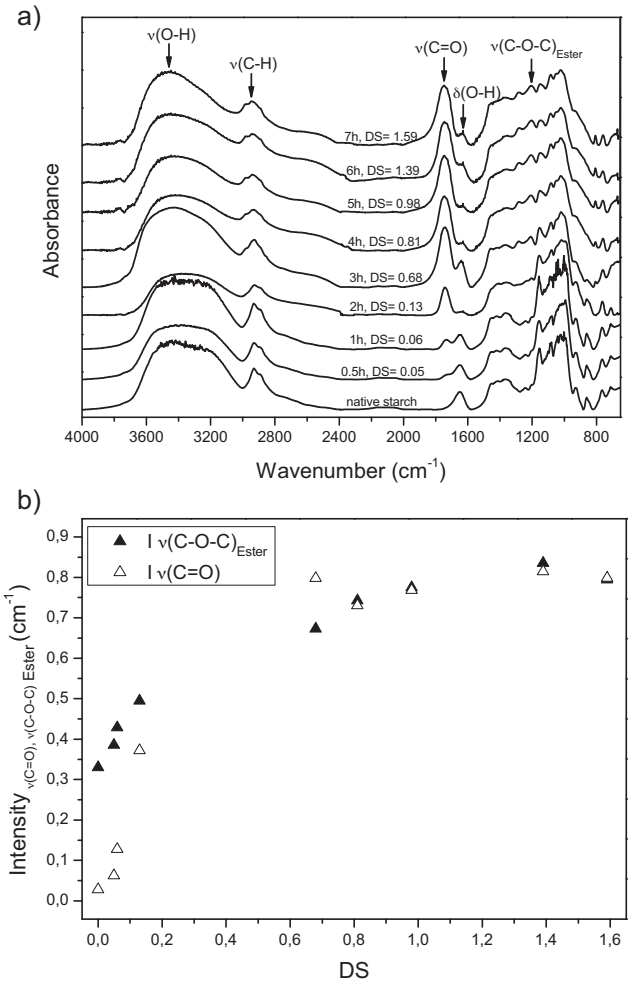

Fig. 3. (a) FTIR spectra of native and propionylated corn starch samples and (b) intensity of characteristic esters bands as a function of DS.

assigned to O—H stretching, two overlapped bands centred at 2930 and 2893 cm^{-1} attributed to C—H stretching modes, a small band centred at 1242 cm^{-1} assignable to CH_2OH (side chain) related mode and C—O—H deformation mode, and highly overlapped bands within the 1200–1000 cm^{-1} region attributed to coupling mode of C—O and C—C stretching, C—O—H bending mode, and C—O stretching. Main absorption bands observed at lower wavenumbers of native starch FTIR spectrum were attributed to skeletal mode vibrations, C—H and CH_2 deformation and C—C stretching vibrations (Cael, Koenig, & Blackwell, 1975; Garg & Jana, 2011; Kizil, Irudayaraj, & Seetharaman, 2002). The band centred at 1649 cm^{-1} was assigned to the O—H bending vibration of adsorbed water molecules.

In accordance with NMR spectra, FTIR spectra of propionylated starches proved esterification by appearance of signals characteristic of propionate groups vibrations. The most important one was the signal assigned to the typical stretching of the carbonyl ester group (C=O), centred at 1736 cm^{-1} for low-substituted samples (i.e. DS = 0.05–0.06) and shifted towards up to 1746 cm^{-1} for the highly acylated samples (i.e. DS = 0.81–1.59). Furthermore the signal at 1205 cm^{-1}, attributed to C—O—C stretching vibration of the ester groups introduced, was also an evidence of esterification. Acetylated starch samples normally show this signal at around 1240–1250 cm^{-1} (Biswas et al., 2008; Hampe & Heinze, 2014; López-Rubio et al., 2009; Tupa et al., 2013, 2015). However, this band is known to shift towards lower wavenumbers for propionate esters (Skoog, Holler, & Nieman, 2001).

The increase of the intensity of ester signals as a function of DS is illustrated in Fig. 3b. As it is shown, the absorbance of signals corresponding to vibrations of propionate groups increased with DS up to DS ≈ 0.7, after which almost constant absorbance values were observed due to signal saturation. Finally, the appearance of a new shoulder centred at 2984 cm^{-1} for samples with DS higher than 0.13 was attributed to stretching vibrations of the C—H groups of the propionate esters introduced.

3.4. Scanning electron microscopy (SEM)

Scanning electron microscopy was used to study the effects of propionylation on starch granules morphology and integrity. As it is shown in Fig. 4a, native corn starch granules are poliedric shape particles with smooth surface and diameters in the 2–20 μm range (Fig. 4a). In the first hours of reaction propionylation, when DS reached 0.05–0.06, starch granules showed a similar aspect, with preserved granular structure (Fig. 4b and c). However, longer reaction times evidenced the progressive fusion and loss of the granular structure of starch (Fig. 4d and e). Fusion/aggregation of esterified starch granules has been previously attributed to partial disruption of their surface as a consequence of the chemical modification procedure (Singh, Kaur, & Singh, 2004), as well as to the introduction of bulky ester groups which disrupted the internal structure and weakened the granule, and also to the effect of heating (Diop et al., 2011).

In the current system, the progressive changes observed for propionylated starches with increasing substitution level are thought to be a consequence not only of the higher content of the bulky propionate groups introduced, but also to the effect of the acid acylant which could have contributed to starch granules disruption. Acidic reagents/catalysts have previously been reported to disrupt the crystalline structure of starch granules (Cheetham & Tao, 1998; Mei, Zhou, Jin, Xu, & Chen, 2015).

However, the disruption of starch granules by the *sole* action of propionic acid during extended periods of time (i.e. with no significant contribution of the average number of OH groups that have been substituted) can be ruled out by comparison of Fig. 4e and f. Fig. 4f corresponds to the uncatalyzed propionylation of corn starch

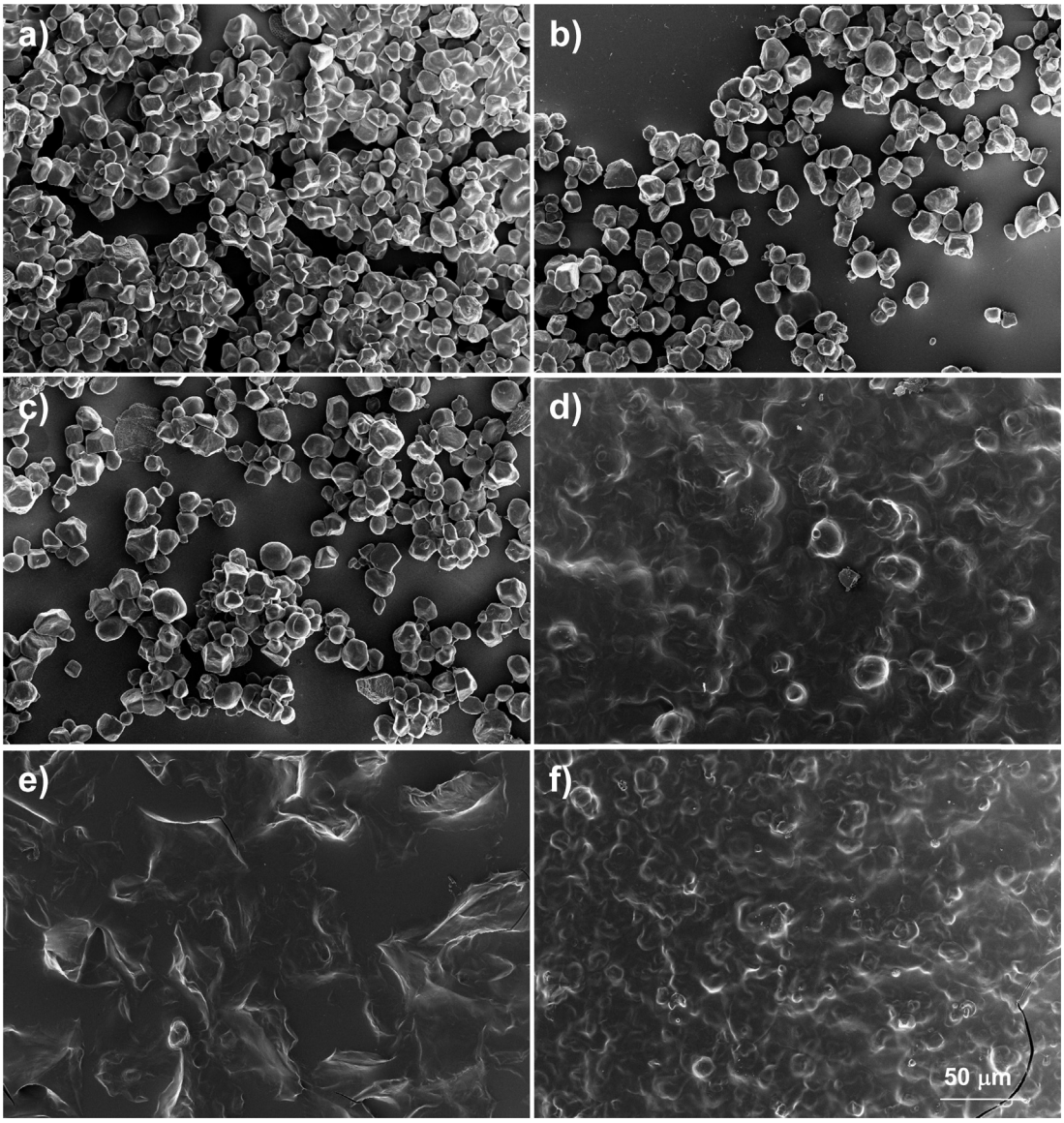

Fig. 4. SEM micrographies of native and propionylated starch with increasing DS, 1KX. (a) Native starch, (b) 0.5 h – DS = 0.05, (c) 1 h – DS = 0.06, (d) 2 h – DS = 0.13, (e) 7 h – DS = 1.59, (f) 7 h uncatalyzed reaction – DS = 0.16.

granules during 7 h at 130 °C with no catalyst addition. Under those conditions the uncatalyzed propionylation of starch led to a DS of 0.16. As it is shown, even if starch granules were exposed to propionic acid/temperature/stirring during the same time interval than those shown in Fig. 4e, the loss of the original shape of starch granules and their re-association to form new bigger irregularly shaped particles evidenced in Fig. 4e (i.e. DS = 1.59), was not observed when the introduction of ester groups was limited to a DS of 0.16. Disruption of starch granules by the sole action of heating or L-tartaric acid presence can also be ruled out since esterification of corn starch with acetic anhydride under analogous conditions did not at all induced the morphological changes herein observed (Tupa et al., 2015).

In terms of the effect of granules fusion/aggregation in their digestion properties, compound granules built from individual granules have been observed to possess a limited degree of hydrolysis as the packing has been reported to reduce the capacity for amylases to bind to granule surfaces (Tester, Qi, & Karkalas, 2006).

3.5. X-ray diffraction (XRD)

Changes in the semicrystalline structure of starch induced by propionylation at increasing DS were investigated by means of X-ray diffraction. Results are shown in Fig. 5. Native corn starch showed an A-type pattern characteristic of cereal starch, with reflections at 2θ: 4.9°, 17.0°, 17.8°, 19.8° and 22.7°. XRD patterns of propionylated starches with the lowest DS values (i.e. 0.05 and 0.06) showed no significant changes with respect to the diffractogram of native starch, which has previously been attributed to chemical modification that has mostly taken place in the amorphous regions of the granules (Chen, Schols, & Voragen, 2004; López-Rubio et al., 2009).

However, and in line with SEM micrographies, further propionylation of starch (i.e. DS = 0.13) significantly affected the polysaccharide structure as evidenced by an important reduction of the intensity of characteristic XRD peaks. The degree of crystallinity in cereal starch has been largely attributed to the formation of double helices by intermolecular hydrogen bonds

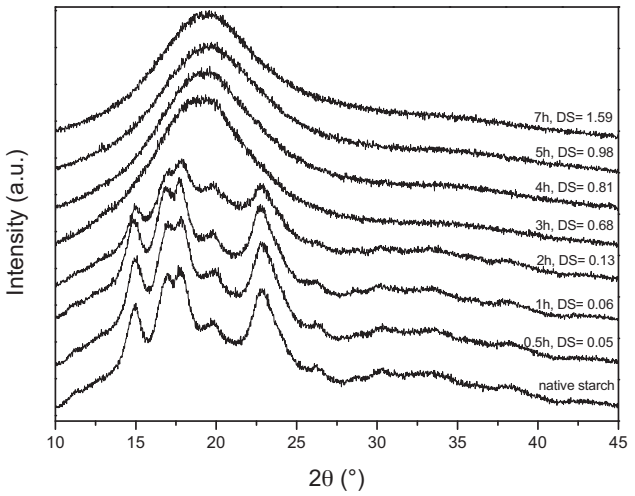

Fig. 5. X-ray diffraction patterns of native and propionylated starch samples.

within the amylopectin segments (Zhang, Xie, Zhao, Liu, & Gao, 2009). Thus, the reduction of crystallinity during esterification has been frequently explained in terms of a lower formation of inter and intramolecular hydrogen bonds, due to the partial replacement hydroxyl groups of starch with more voluminous hydrophobic ester groups (Diop et al., 2011; Zhang et al., 2009). Besides introduction of bulky and hydrophobic ester groups, and as hypothesized in the previous section, the acid acylant might have contributed to the disruption of starch granules. Disruption of the crystalline domains of starch granules by acid reagents such as citric acid and iodine has previously been reported (Cheetham & Tao, 1998; Mei et al., 2015).

Furthermore, for DS ≥ 0.68, propionylated starches showed a totally amorphous diffraction diagram, with a wide peak centred at $2\theta = 19^{\circ}$. Diffractograms of highly substituted acetylated, propionylated and butyrylated starch have previously shown the observed behaviour with typical wide peaks near 6–9° and 20° (2θ) indicating an amorphous pattern (Chi et al., 2008; Garg & Jana, 2011).

At this point, characterization results obtained from XRD and SEM give insight on the evolution of reaction with time illustrated in Fig. 1. The derivatization pattern within starch granules has previously been reported to be dependent on the relative crystallinity of its regions, with derivatization starting/preferentially occurring in the amorphous regions of the granules, and proceeding then to the more crystalline zones (Gray & BeMiller, 2004). Moreover, under heterogeneous conditions, the peripheral hydroxyl groups and glucose residues in the granular starch are expected to be preferentially esterified over the inner core of the granule with less accessibility of the acylant reagent (and herein also of the dissolved catalyst) (Chen et al., 2004; Diop et al., 2011; Yang & Montgomery, 2006). In Fig. 1 the evolution of reaction did not evidence a reduction of reaction velocity which could be ascribed to the described heterogeneity of starch granules. Instead, after 2 h of reaction (i.e. DS = 0.13), derivatization rate noticeably increased which correlated with the disruption of starch granules and their significant reduction in crystallinity determined for this time interval/DS from SEM and XRD data.

3.6. Thermogravimetric analysis (TGA)

Changes on the thermal stability of corn starch upon propionylation were assessed as a function of DS when heated at a constant rate (10 °C/min) in the 25–800 °C range. Data in terms of the first derivative of TG signals (DTG) normalized with respect to the initial sample mass are presented in Fig. 6a moved in the *y* axes for clarity purposes. Fig. 6b–d illustrates the evolution of T_{onset} (calculated as the intersection of the extrapolated pre-decomposition ordinate value and a tangential line drawn to the point of steepest slope of the weight loss curve in the decomposition region), T_{max} (temperature of maximum weight loss rate), and residual moisture content retained in preconditioned samples (105 °C, 2 h), as a function of DS.

DTG analysis (Fig. 6a) of native corn starch showed two peaks corresponding to two weight losses, the first one (from room temperature to ≈130 °C) associated with the polysaccharide dehydration, and the second one (T_{onset} = 309 °C, T_{max} = 326 °C) assigned to the thermal decomposition of starch as a result of the inter- and intramolecular dehydration reactions with water as the main product of decomposition (Thiebaud et al., 1997). Propionylated starches with low DS (i.e. DS = 0.05–0.06) showed slightly lower T_{onset} and T_{max} values, i.e. 296 °C and 319 °C, respectively. However, propionylated starches with DS in the 0.13–1.59 interval showed a much significant reduction in thermal stability as illustrated by T_{onset} and T_{max} values within the 260–254 °C and 299–286 °C intervals, respectively (Fig. 6b–d). The reduction in thermal stability of propionylated starches with DS ≥ 0.13 is in line with the important loss of crystalline order deduced from XRD data.

In previous contributions dealing with the thermal decomposition properties of esterified starches, both reduction and also increase in the thermal stability of the polysaccharide upon acylation have been reported. In the contribution of Garg and Jana (2011) dealing with the propionylation of corn starch with the corresponding anhydride after preactivation with pyridine, authors reported that acylated starch was thermally more stable upon esterification, with decomposition temperature intervals which moved to higher temperatures for increasing DS values (i.e. 250–350 °C for native starch, 279–382 °C for DS = 0.61 and 300–400 °C for DS = 2.41). Authors attributed the observed pattern to the low amount of remaining hydroxyl groups in starch molecule after modification and to the increase in molecular weight and covalent bonding due to the acylation. On the other hand, Cyras, Tolosa Zenklusen, and Vazquez (2006) reported that their esterified starches were less thermally stable than native starch, which they assigned to the reduction in the number of OH groups and the addition of a voluminous group which, as in the present case, produced a lower crystallinity value. TG results herein obtained correlated with the conclusions drawn from SEM and XRD which indicated that the esterification process progressively transformed semicrystalline structure of starch granules into an amorphous structure, which could have in turn accelerated the thermal decomposition of starch (Lin, Li, Long, Su, & Huang, 2014; Lu, Luo, Yu, & Fu, 2012).

Finally, the evolution of the moisture content remaining in propionylated samples with increasing DS is illustrated in Fig. 6d. As it is shown, the physically adsorbed and hydrogen bond linked water percentage remaining in starch after preconditioning (105 °C, 2 h) significantly decreased with increasing DS (i.e. 6.6% for native starch, 4.3% for DS = 0.05–0.06, 2.1% for DS = 0.13 and 1.2–1.6% for higher DS); evidencing the reduction in starch hydrophilicity when hydroxyl groups were progressively replaced by less hydrophilic propionate groups. Similar results have previously been informed for propionylated cassava starch samples with increasing DS (Santayanon & Wootthikanokkhan, 2003).

3.7. Hydrophobicity test

Given the expected change in the polarity of esterified starch samples upon replacement of hydrophilic OH groups with less polar ester groups, starch propionates were qualitatively tested for hydrophobicity in test tubes containing equal volumes of distilled water and petroleum ether (0.67 g/mL). When poured into the biphasic system, native starch was observed to fall to the lower aqueous phase, and remain confined within it in spite of vigorous

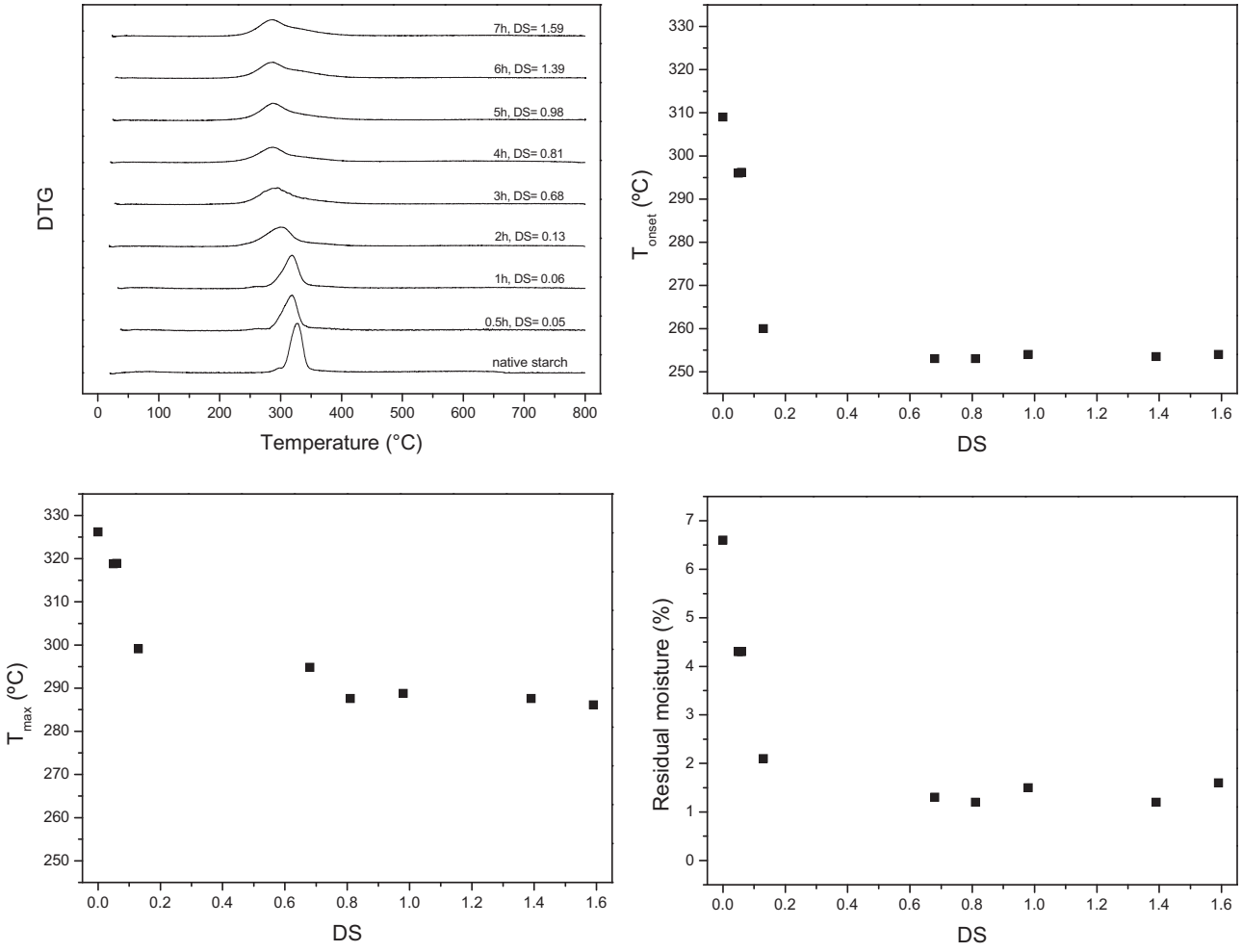

Fig. 6. (a) DTG, (b) T_{onset}, (c) T_{max} and (d) residual mositure content values as a function of the DS of propionylated starch samples.

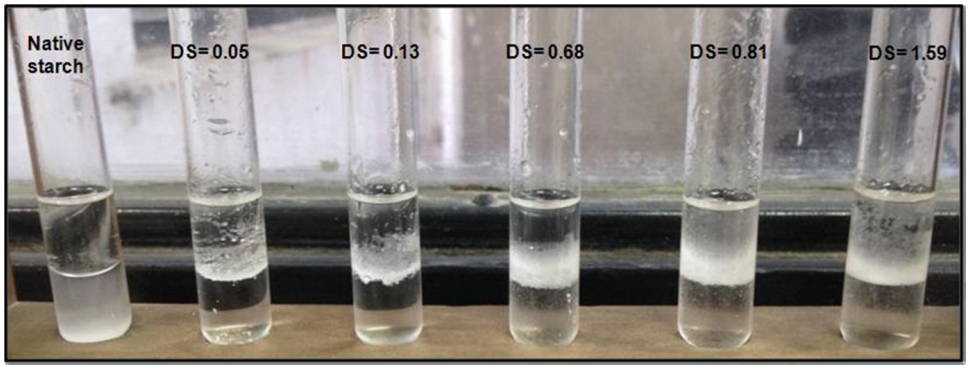

Fig. 7. Distribution of native and propionylated starch samples within biphasic liquid systems distilled water/petroleum ether.

vertical shaking. On the other hand, and irrespectively of the samples DS, starch propionates preferentially remained in the lowest zone of the upper organic phase and never got to the bulk aqueous phase. Fig. 7 illustrates the described distribution of the derivatized starch samples within the biphasic system, qualitatively confirming the change in starch hydrophilicity after propionylation.

4. Conclusions

A non-conventional organocatalytic solventless route for the eco-friendly synthesis of propionylated starch with varying DS was proposed. Propionylation of corn starch was catalyzed by L-tartaric acid, a naturally occurring α-hydroxy acid. Propionylated starches with degree of substitution (DS) in the 0.05–1.59 interval were obtained and characterized in terms of chemical structure, morphology, crystallinity, thermal stability and hydrophilicity.

^{13}C CP-MAS NMR and FTIR spectroscopy confirmed the successful propionylation of starch by appearance of signals characteristic of the ester groups introduced. On the other hand, SEM and XRD results gave insight on the progressive disruption and loss of crystallinity of starch granules for increasing DS values, which was attributed to both the acid acylant effect and the progressive

replacement of hydroxyls with bulky hydrophobic propionyl groups. Conversion of the semi-crystalline organization of starch into an amorphous structure had a significant impact on the susceptibility of starch granules to chemical modification, with derivatization rate significantly increasing for DS values for which characterization results indicated the loss of crystalline order (DS > 0.13). Crystallinity changes also correlated with a reduction of thermal stability of acylated samples. The derivatization route introduced proved useful to significantly reduce the hygroscopicity and hydrophilicity of starch and enhance its compatibility with non-polar media.

In terms of propionylated starch uses, by use of the organocatalytic methodology herein proposed acylated starches with the DS required for clinical application (i.e. delivery of specific SCFA to the colon) could be obtained within 2–3 h of reaction, a time interval much lower than those previously reported for other synthetic routes. Besides, for propionylated starches with such low DS (for which no significant disruption/solubilization of granules was observed), easy recovery and reuse of propionic acid + dissolved tartaric acid by direct filtration, appear as a promising possibility for reducing operations costs, specially at higher scale.

Acknowledgements

Authors acknowledge Consejo Nacional de Investigaciones Científicas y Técnicas (PIP 11220110100608) and Agencia Nacional de Promoción Científica y Tecnológica for financial support (PICT 1957 2012 – PRESTAMO BID). Authors are also thankful to Lic. Silvana Arroyo (INTECIN-UBA) for XRD data acquisition.

References

Adebowale, K. O., Afolabi, T. A., & Lawal, O. S. (2002). Isolation, chemical modification and physicochemical characterisation of Bambarra groundnut (*Voandzeia subterranean*) starch and flour. *Food Chemistry*, *78*, 305–311.

Annison, G., Illman, R. J., & Topping, D. L. (2003). Acetylated, propionylated or butyrylated starches raise large bowel short chain fatty acids preferentially when fed to rats. *Journal of Nutrition*, *133*, 3523–3528.

Asp, N. G. (1992). Resistant starch. *European Journal of Clinical Nutrition*, *46*(Suppl. 2), S1.

Bajka, B. H. (2007). *The effects of increased butyrate delivered as butyrylated starch on large bowel physiology in the rat* (Ph.D. thesis). University of Adelaide.

Betancur, A. D., Chel, G. L., & Canizares, H. E. (1997). Acetylation and characterization of *Canavalia ensiformis* starch. *Journal of Agricultural and Food Chemistry*, *45*, 378–382.

Biswas, A., Shogren, R. L., Selling, G., Salch, J., Willett, J. L., & Buchanan, C. M. (2008). Rapid and environmentally friendly preparation of starch esters. *Carbohydrate Polymers*, *74*, 137–141.

Bushra, M., Yun, X. X., Pan, S. Y., Hydamaka, A., Hua, M. W., & Feng, W. L. (2013). Effect of oxidation and esterification on functional properties of mung bean (*Vigna radiata* (L.) Wilczek) starch. *European Food Research and Technology*, *236*, 119–128.

Cael, J. J., Koenig, J. L., & Blackwell, J. (1975). Infrared and Raman spectroscopy of carbohydrates. Part VI: Normal coordinate analysis of V-amylose. *Biopolymers*, *14*, 1885–1903.

Cheetham, N. W. H., & Tao, L. (1998). Solid state NMR studies on the structural and conformational properties of natural maize starches. *Carbohydrate Polymers*, *36*, 283–292.

Chen, Z. H., Schols, H. A., & Voragen, A. G. J. (2004). Differently sized granules from acetylated potato and sweet potato starches differ in the acetyl substitution pattern of their amylose populations. *Carbohydrate Polymers*, *56*, 219–226.

Cherbut, C. (2002). Inulin and oligofructose in the dietary fibre concept. *British Journal of Nutrition*, *87*(Suppl. 2), 159–162.

Chi, H., Xu, K., Wu, X., Chen, Q., Xue, D., Song, C., et al. (2008). Effect of acetylation on the properties of corn starch. *Food Chemistry*, *106*, 923–928.

Clarke, J. M., Bird, A. R., Topping, D. L., & Cobiac, L. (2007). Excretion of starch and esterified short-chain fatty acids by ileostomy subjects after the ingestion of acylated starches. *American Journal of Clinical Nutrition*, *86*, 1146–1151.

Clarke, J. M., Young, G. P., Topping, D. L., Bird, A. R., Cobiac, L., Scherer, B. L., et al. (2012). Butyrate delivered by butyrylated starch increases distal colonic epithelial apoptosis in carcinogen-treated rats. *Carcinogenesis*, *33*, 197–202.

Cyras, V. P., Tolosa Zenklusen, M. C., & Vazquez, A. (2006). Relationship between structure and properties of modified potato starch biodegradable films. *Journal of Applied Polymer Science*, *101*, 4313–4319.

Diop, C. I. K., Li, H. L., Xie, B. J., & Shi, J. (2011). Effects of acetic acid/acetic anhydride ratios on the properties of corn starch acetates. *Food Chemistry*, *126*, 1662–1669.

Garg, A., & Jana, A. K. (2011). Characterization and evaluation of acylated starch with different acyl groups and degrees of substitution. *Carbohydrate Polymers*, *83*, 1623–1630.

Gray, J. A., & BeMiller, J. N. (2004). Development and utilization of reflectance confocal laser scanning microscopy to locate reaction sites in modified starch granules. *Cereal Chemistry*, *81*, 278–286.

Hampe, R., & Heinze, T. (2014). Studies about the solvent-dependent substitution pattern of starch acetates. *Macromolecular Materials and Engineering*, *299*(10), 1188–1196.

Han, F., Gao, C., Liu, M., Huang, F., & Zhang, B. (2013). Synthesis, optimization and characterization of acetylated corn starch with the high degree of substitution. *International Journal of Biological Macromolecules*, *59*, 372–376.

Kaur, B., Ariffin, F., Bhat, R., & Karim, A. A. (2012). Progress in starch modification in the last decade. *Food Hydrocolloids*, *26*, 398–404.

Kizil, R., Irudayaraj, J., & Seetharaman, K. (2002). Characterization of irradiated starches by using FT-Raman and FTIR spectroscopy. *Journal of Agricultural and Food Chemistry*, *50*, 3912–3918.

Lin, R., Li, H., Long, H., Su, J., & Huang, W. (2014). Synthesis of rosin acid starch catalyzed by lipase. *BioMed Research International*, 1–8.

López-Rubio, A., Clarke, J. M., Scherer, B., Topping, D., & Gilbert, E. P. (2009). Structural modifications of granular starch upon acylation with short-chain fatty acids. *Food Hydrocolloids*, *23*, 1940–1946.

Lu, X., Luo, Z., Yu, S., & Fu, X. (2012). Lipase-catalyzed synthesis of starch palmitate in mixed ionic liquids. *Journal of Agricultural and Food Chemistry*, *60*, 9273–9279.

Mei, J.-Q., Zhou, D.-N., Jin, Z.-Y., Xu, X.-M., & Chen, H.-Q. (2015). Effects of citric acid esterification on digestibility, structural and physicochemical properties of cassava starch. *Food Chemistry*, *187*, 378–384.

Morán, J. I., Cyras, V. P., & Vazquez, A. (2013). Preparation and characterization of three different derivatized potato starches. *Journal of Polymers and the Environment*, *21*, 395–404.

Morita, T., Kasaoka, S., Kiriyama, S., Brown, I. L., & Topping, D. L. (2005). Comparative effects of acetylated and unmodified high-amylose maize starch in rats. *Starch*, *57*, 246–253.

Nugent, A. P. (2005). Health properties of resistant starch. *British Nutrition Foundation, Nutrition Bulletin*, *30*, 27–54.

Paris, M., Bizot, H., Emery, J., Buzaré, J. Y., & Buléon, A. (1999). Crystallinity and structuring role of water in native and recrystallized starches by ^{13}C CP-MAS NMR spectroscopy. 1: Spectral decomposition. *Carbohydrate Polymers*, *39*, 327–339.

Paris, M., Bizot, H., Emery, J., Buzaré, J. Y., & Buléon, A. (2001). NMR local range investigations in amorphous starchy substrates. I. Structural heterogeneity probed by ^{13}C CP-MAS NMR. *International Journal of Biological Macromolecules*, *29*, 127–136.

Sandhu, K. S., Kaur, M., Singh, N., & Lim, S. T. (2008). A comparison of native and oxidized normal and waxy corn starches: Physicochemical, thermal, morphological and pasting properties. *LWT – Food Science and Technology*, *41*, 1000–1010.

Santayanon, R., & Wootthikanokkhan, J. (2003). Modification of cassava starch by using propionic anhydride and properties of the starch-blended polyester polyurethane. *Carbohydrate Polymers*, *51*, 17–24.

Shin, S. I., Lee, Ch. J., Kim, M. J., Choi, H. J., Kim, Y., et al. (2009). Structural characteristics of low-glycemic response rice starch produced by citric acid treatment. *Carbohydrate Polymers*, *78*, 588–595.

Singh, N., Chawla, D., & Singh, J. (2004). Influence of acetic anhydride on physicochemical, morphological and thermal properties of corn and potato starch. *Food Chemistry*, *86*, 601–608.

Singh, J., Kaur, L., & Singh, N. (2004). Effect of acetylation on some properties of corn and potato starches. *Starch/Stärke*, *56*(12), 586–601.

Skoog, D. A., Holler, F. J., & Nieman, T. A. (2001). *Principios de análisis instrumental* (5th ed.). España: Concepción Fernández Madrid (Chapter 16).

Tang, H., & Hills, B. P. (2003). Use of ^{13}C MAS NMR to study domain structure and dynamics of polysaccharides in the native starch granules. *Biomacromolecules*, *4*, 1269–1276.

Tester, R. F., Qi, X., & Karkalas, J. (2006). Hydrolysis of native starches with amylases. *Animal Feed Science and Technology*, *130*, 39–54.

Thiebaud, S., Aburto, J., Alric, I., Borredon, E., Bikiaris, D., Prinos, J., et al. (1997). Properties of fatty-acid esters of starch and their blends with LDPE. *Journal of Applied Polymer Science*, *65*, 705–721.

Topping, D. L., & Clifton, P. M. (2001). Short-chain fatty acids and human colonic function: Roles of resistant starch and nonstarch polysaccharides. *Physiological Reviews*, *81*, 1031–1064.

Tupa, M., Maldonado, L., Vázquez, A., & Foresti, M. L. (2013). Simple organocatalytic route for the synthesis of starch esters. *Carbohydrate Polymers*, *98*, 349–357.

Tupa, M. V., Ávila Ramírez, J. A., Vázquez, A., & Foresti, M. L. (2015). Organocatalytic acetylation of starch: Effect of reaction conditions on DS and characterisation of esterified granules. *Food Chemistry*, *170*, 295–302.

Wang, X., Gao, W. Y., Zhang, L. M., Xiao, P. G., Yao, L. P., Liu, Y., et al. (2008). Study on the morphology, crystalline structure and thermal properties of yam starch

acetates with different degrees of substitution. *Science in China Series B – Chemistry*, *51*(9), 859–865.
West, N. P., Christophersen, C. T., Pyne, D. B., Cripps, A. W., Conlon, M. A., Topping, D. L., et al. (2013). Butyrylated starch increases colonic butyrate concentration but has limited effects on immunity in healthy physically active individuals. *Exercise Immunology Review*, *19*, 102–119.
Yang, B. Y., & Montgomery, R. (2006). Acylation of starch using trifluoroacetic anhydride promoter. *Starch/Stärke*, *58*, 520–526.
Zhang, L. M., Xie, W. G., Zhao, X., Liu, Y., & Gao, W. (2009). Study on the morphology, crystalline structure and thermal properties of yellow ginger starch acetates with different degrees of substitution. *Thermochimica Acta*, *495*, 57–62.